Measurement of the branching fraction of $\psi(3686) \to \omega\eta\eta$

M. Ablikim *et al.*[*]

(BESIII Collaboration)

Using a sample of $(2.712 \pm 0.014) \times 10^9$ $\psi(3686)$ events collected with the BESIII detector at the BEPCII collider in 2009, 2012, and 2021, the decay $\psi(3686) \to \omega\eta\eta$ is observed for the first time. The branching fraction of the $\psi(3686) \to \omega\eta\eta$ decay is measured to be $(1.65 \pm 0.02 \pm 0.21) \times 10^{-5}$, where the first uncertainty is statistical and the second systematic.

I. INTRODUCTION

Charmonium states such as J/ψ and $\psi(3686)$ lie between the perturbative and nonperturbative regimes of quantum chromodynamics (QCD) [1], which describes strong interactions between quarks and gluons. Although QCD has achieved remarkable successes in the perturbative regime, its behavior in the nonperturbative regime, such as color confinement and hadronization process, remains one of the challenges in particle physics. Experimental studies of charmonium hadronic decays are therefore essential for testing QCD calculations derived from various phenomenological models [2,3]. Moreover, although the current QCD framework describes almost all observed hadrons, several predicted states have yet to be discovered.

In recent years, many multibody light hadron decays of $\psi(3686)$ have been studied [4]. However, no experimental study of $\psi(3686) \to \omega\eta\eta$ has been reported. Investigating $\psi(3686) \to \omega\eta\eta$ also offers an opportunity to search for excited states in the $\omega\eta$ and $\eta\eta$ mass distributions, e.g., $\omega(1420)$, $h_1(1380)$, and $h_1(2300)$ [5], as well as for other possible excited ω and h_1 states. In this paper, we present the first measurement of the branching fraction of $\psi(3686) \to \omega\eta\eta$ based on $(2.712 \pm 0.014) \times 10^9$ $\psi(3686)$ events [6] collected with the BESIII detector at the BEPCII collider in 2009, 2012, and 2021.

II. THE BESIII DETECTOR AND MONTE CARLO SAMPLES

The BESIII detector [7] records symmetric e^+e^- collisions provided by the BEPCII storage ring [8] in the center-of-mass energy range from 1.84 to 4.95 GeV. The cylindrical core of the BESIII detector covers 93% of the full solid angle and consists of a helium-based multilayer drift chamber (MDC), time-of-flight system (TOF), and a CsI(Tl) electromagnetic calorimeter (EMC) which are all enclosed in a superconducting solenoidal magnet providing a 1.0 T magnetic field. Modules of the resistive plate muon counter (MUC) are embedded in an octagonal flux-return yoke that supports the superconducting solenoid. The charged-particle momentum resolution at 1 GeV/c is 0.5%, and the specific ionization energy loss dE/dx resolution is 6% for electrons from Bhabha scattering at 1 GeV. The EMC measures photon energies with a resolution of 2.5% (5%) at 1 GeV in the barrel (end cap) region. The time resolution in the plastic scintillator TOF barrel region is 68 ps, while that in the end cap region was 110 ps. The end cap TOF system was upgraded in 2015 using multigap resistive plate chamber technology, providing a time resolution of 60 ps, which benefits 83% of the data used in this analysis [9–11].

Monte Carlo (MC) simulated data samples produced with a GEANT4-based [12] software package, which includes the geometric description [13] of the BESIII detector and the detector response, are used to determine detection efficiencies and to estimate backgrounds. The simulation models the beam energy spread and initial state radiation (ISR) in the e^+e^- annihilations with the generator KKMC [14,15]. The inclusive MC sample includes the production of the $\psi(3686)$ resonance, the ISR production of the J/ψ and the continuum processes incorporated in KKMC. Particle decays are generated by EVTGEN [16,17] for the known decay modes with branching fractions taken from the Particle Data Group (PDG) [4] and by LUNACHARM [18,19] for the unknown ones. Final-state radiation from charged final-state particles is included using the PHOTOS package [20]. To evaluate the detection efficiencies and optimize the event selection criteria, a signal MC sample of $\psi(3686) \to \omega\eta\eta$, comprising 0.2 million events, is generated with a uniform phase space (PHSP) distribution.

---

[*]Full author list given at the end of the article.

III. EVENT SELECTION

The ω and η mesons are reconstructed via $\omega \to \pi^+\pi^-\pi^0$ and $\eta \to \gamma\gamma$, respectively. Events are required to contain two oppositely charged tracks and at least six photon candidates. Charged tracks detected in the MDC are required to be within a polar angle (θ) range of $|\cos\theta| < 0.93$, where θ is defined with respect to the detector symmetry axis (z-axis), and their distance of closest approach to the interaction point must be less than 10 cm along the z-axis and less than 1 cm in the transverse plane. Particle identification (PID) for charged tracks combines measurements of dE/dx and the flight time in the TOF to form likelihoods $\mathcal{L}_h$ ($h = p, K, \pi$) for each hadron h hypothesis. Tracks are identified as pions when the pion hypothesis has the greatest likelihood, i.e., $\mathcal{L}_\pi > \mathcal{L}_K$ and $\mathcal{L}_\pi > \mathcal{L}_p$. Exactly one $\pi^+\pi^-$ pair is required. Photon candidates are identified using showers in the EMC. The deposited energy of each shower is more than 25 MeV in the barrel region ($|\cos\theta| < 0.80$) and more than 50 MeV in the end cap region ($0.86 < |\cos\theta| < 0.92$). To exclude showers induced by charged particles, the angle between the position of each shower in the EMC and the closest extrapolated charged track is required to be larger than 10°. To suppress electronic noise and showers unrelated to the event, the difference between the EMC time and the event start time is required to be within [0,700] ns.

To improve momentum resolution and suppress background, a four-constraint (4C) kinematic fit imposing energy-momentum conservation under the $\psi(3686) \to \pi^+\pi^-6\gamma$ hypothesis is applied. For events with more than six photon candidates, the combination with the smallest χ^2_{4C} of the 4C kinematic fit is retained, and $\chi^2_{4C} < 40$ is required. This requirement is determined by optimizing the figure-of-merit (FOM), defined as: $\text{FOM} = S/\sqrt{S + B}$, where S represents the number of signal events from the signal MC sample and B represents the number of background events from the inclusive MC sample. π^0 and η candidates are selected by minimizing $\chi^2_{\pi^0\eta\eta} = \frac{(M(\gamma_1\gamma_2)-m_{\pi^0})^2}{\sigma^2_{\pi^0}} + \frac{(M(\gamma_3\gamma_4)-m_\eta)^2}{\sigma^2_\eta} + \frac{(M(\gamma_5\gamma_6)-m_\eta)^2}{\sigma^2_\eta}$, where m_{π^0} and m_η are the nominal masses of π^0 and η [4], σ_{π^0} and σ_η are their corresponding resolutions estimated by the signal MC sample, respectively. The π^0 and η candidates are then required to be within $|M(\gamma_1\gamma_2) - m_{\pi^0}| < 20$ MeV/c^2, $|M(\gamma_3\gamma_4) - m_\eta| < 25$ MeV/c^2 and $|M(\gamma_5\gamma_6) - m_\eta| < 25$ MeV/c^2. The ω signal is derived from the distribution of the $\pi^+\pi^-\pi^0$ invariant mass $M(\pi^+\pi^-\pi^0)$.

To suppress the backgrounds with one or two additional photons, additional 4C kinematic fits under the hypotheses of $\psi(3686) \to \pi^+\pi^-7\gamma$ and $\psi(3686) \to \pi^+\pi^-8\gamma$ are performed. Events with χ^2_{4C} smaller than that of the signal hypothesis are discarded. In order to remove the backgrounds from $\psi(3686) \to \pi^+\pi^-\pi^0\pi^0\eta$,

$\psi(3686) \to \pi^+\pi^-\pi^0\pi^0\pi^0$, and $\psi(3686) \to \pi^+\pi^-\eta\eta$, three χ^2 functions analogous to $\chi^2_{\eta\eta\pi^0}$ are defined for the $\pi^0\pi^0\eta$, $\pi^0\pi^0\pi^0$, and $\eta\eta\eta$. We require $\chi^2_{\eta\eta\pi^0} < \chi^2_{\pi^0\pi^0\eta}$, $\chi^2_{\eta\eta\pi^0} < \chi^2_{\pi^0\pi^0\pi^0}$, and $\chi^2_{\eta\eta\pi^0} < \chi^2_{\eta\eta\eta}$. To suppress the backgrounds containing two π^0 mesons, the $\chi^2_{\pi^0\pi^0}$ is defined to select one π^0 pair, and the requirements of $|M(\gamma_1\gamma_2) - m_{\pi^0}| > 0.03$ GeV/c^2 and $|M(\gamma_3\gamma_4) - m_{\pi^0}| > 0.03$ GeV/c^2 are applied. Additionally, to suppress the backgrounds from $\psi(3686) \to \pi^+\pi^-J/\psi$ and $J/\psi \to \omega\eta$, a requirement of $|M(\pi^+\pi^-)_{\text{recoil}} - M_{J/\psi}| > 0.02$ GeV/c^2 is applied. Furthermore, a requirement on the invariant mass of $\omega\eta$, $|M(\omega\eta) - M_{J/\psi}| > 0.03$ GeV/c^2, is used to suppress the backgrounds from $\psi(3686) \to XJ/\psi$, $J/\psi \to \omega\eta$ (X represents other particles).

Potential backgrounds are studied using the inclusive MC sample. No significant peaking background is observed in the $M(\pi^+\pi^-\pi^0)$ distribution. Therefore, the two-dimensional $\eta\eta$ sideband is used to estimate the yield of background from data by combining the background events in the one-dimensional η sideband regions $[0.450, 0.500]$ GeV/c^2 and $[0.594, 0.644]$ GeV/c^2, which are illustrated by the color solid boxes in Fig. 1(a). The normalization factor for the event yields in the one-dimensional η sideband region is obtained from the fit to the distribution of the $\gamma\gamma$ invariant mass $M(\gamma\gamma)$, where the signal is described by a double-Gaussian function and the background by a linear function. The fit results are shown in Figs. 1(b) and 1(c).

To estimate the background contribution from continuum production, we perform the same analysis on the data sample taken at $\sqrt{s} = 3.773$ GeV, corresponding to an integrated luminosity of 2.93 fb^{-1}. Here, it is assumed that the continuum production component completely dominates at this center-of-mass energy. After luminosity scaling, the number of background events from continuum production in the $\psi(3686)$ data is determined.

IV. BRANCHING-FRACTION DETERMINATION

The signal shape is the MC template convolved with a Gaussian, which the mean and sigma values are 0.3 MeV/c^2 and 0.5 MeV/c^2 respectively, accounting for resolution differences; the background is described by a second-order Chebyshev polynomial, while non-η background is taken from the two-dimensional $\eta_H - \eta_L$ sideband. Here, smoothing of the η-η sideband histogram is performed with the RooHistPdf [21]. Throughout this paper, the lower scripts H and L denote the η candidates with higher and lower momenta, respectively. Figure 2 shows the fit result. The resulting signal yield of $\psi(3686) \to \omega\eta\eta$ is determined to be $N_{\text{sig}} = N_{\text{fit}} - N_{\text{con}} = 1251.0 \pm 46.5$. Here, $N_{\text{fit}} = 1274.0 \pm 46.0$ is the fitted number of events, and $N_{\text{con}} = 23.0 \pm 7.0$ is the normalized number of background events from continuum production.
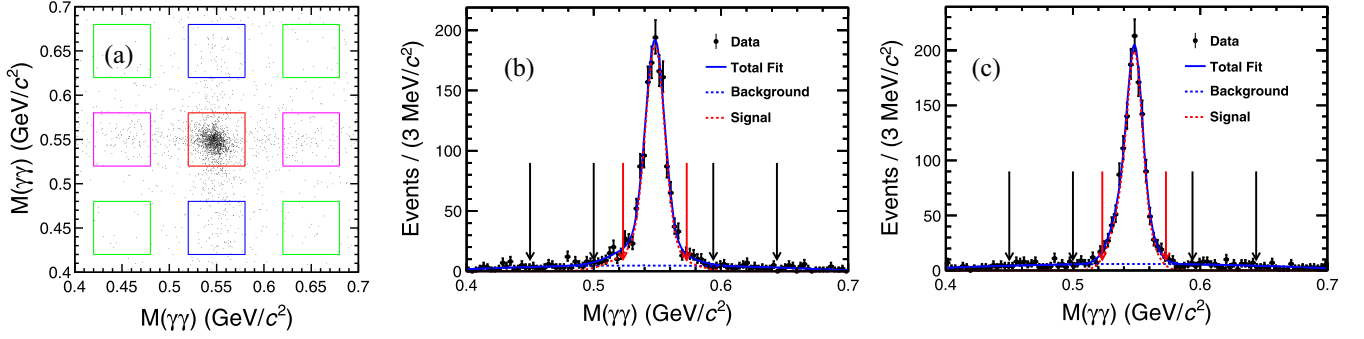
FIG. 1. (a) The distribution of $M(\gamma_3\gamma_4)$ versus $M(\gamma_5\gamma_6)$, where the red box indicates events with η_H and η_L candidates; the blue boxes indicate events with non-η_L candidates; the pink boxes indicate events with non-η_H candidates; and the green box indicates events with non-η_H and non-η_L candidates. (b), (c) The distributions of $M(\gamma_3\gamma_4)$ and $M(\gamma_5\gamma_6)$, where the dots with error bars are the $\psi(3686)$ data; the red dashed line represents the signal, the blue dashed line represents the fitted background, the solid blue line represents the total fit; and the red and black arrows mark the signal and sideband regions, respectively.

The branching fraction of $\psi(3686) \rightarrow \omega\eta\eta$ is calculated by

$$\mathcal{B}(\psi(3686) \rightarrow \omega\eta\eta) = \frac{N_{\mathrm{sig}}}{N_{\psi(3686)} \cdot \varepsilon \cdot \mathcal{B}_1 \cdot \mathcal{B}_2^2 \cdot \mathcal{B}_3}, \quad (1)$$

where $N_{\psi(3686)}$ is the total number of $\psi(3686)$ events in data; $\mathcal{B}_1$, $\mathcal{B}_2$, and $\mathcal{B}_3$ are the branching fractions of $\omega \rightarrow \pi^+\pi^-\pi^0$, $\eta \rightarrow \gamma\gamma$, and $\pi^0 \rightarrow \gamma\gamma$ quoted from the PDG [4], respectively; $\epsilon = 21\%$ is the detection efficiency, based on the simulation of PHSP signal MC and weighted with respect to the distributions of data. Here, the weighting variables are the four-momenta of ω, η and η. Finally, we obtain $\mathcal{B}(\psi(3686) \rightarrow \omega\eta\eta) = (1.65 \pm 0.02) \times 10^{-5}$, where the uncertainty is statistical only.

V. STUDY OF INTERMEDIATE STATES

The Dalitz plot of $M^2(\omega\eta_L)$ versus $M^2(\eta_H\eta_L)$ from the data sample is presented in Fig. 3. The distributions of $M(\omega\eta_H)$ and $M(\eta_H\eta_L)$ are examined as shown in Fig. 4. The photons from η_H are labeled as γ_3 and γ_4, while those from η_L are labeled as γ_5 and γ_6.

Clear accumulation of events is observed around 1.4 GeV/c^2 in the $M(\omega\eta)$ mass spectrum and around 1.7 GeV/c^2 in the $M(\eta\eta)$ mass spectrum, suggestive of the presence of $\omega(1420)$ and $f_0(1710)$. A partial wave analysis (PWA) was performed to generate signal Monte Carlo events for efficiency extraction. The amplitudes of the quasitwo-body decays in the sequential decays are constructed using covariant tensor amplitudes [22]. This analysis included the decay processes $\omega(1420)\eta$, $\omega(1650)\eta$, $h_1(1380)\eta$, $h_1(1595)\eta$, $h_1(1960)\eta$, and $\omega f_0(1710)$, all of which have statistical significances exceeding 5σ. The intermediate states are parametrized by a relativistic Breit-Wigner formula, with mass and width fixed to the values from the PDG [4]. The complex coupling constants of the amplitudes are determined by an unbinned maximum likelihood fit.
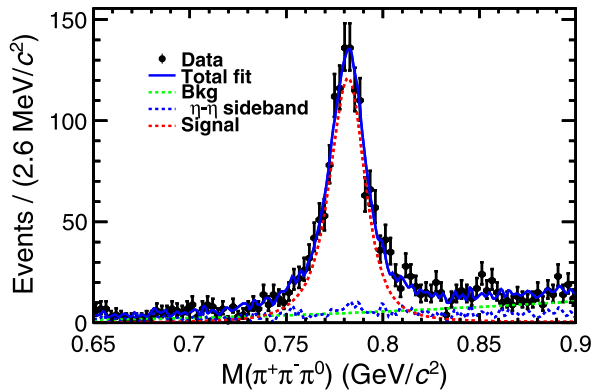

FIG. 2. The fit to the distribution of $M(\pi^+\pi^-\pi^0)$, where the dots with error bars are the $\psi(3686)$ data, the blue curve is the fit result, the red dotted curve is the ω signal, the green dotted curve is the background described by a 2-order polynomial function, and the blue dotted curve is the background derived from events in the two-dimensional sideband regions of $\eta_H - \eta_L$ in data.
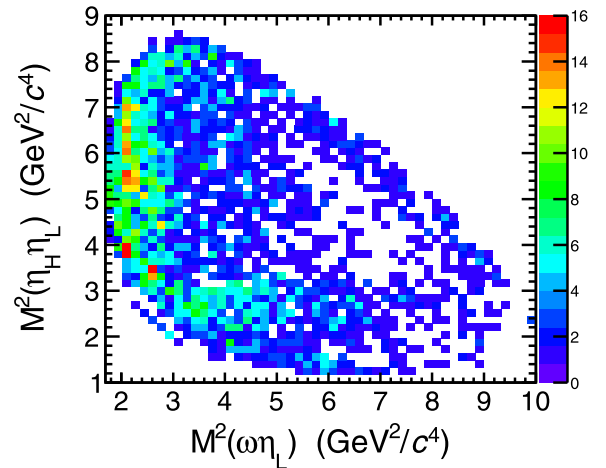

FIG. 3. The Dalitz plot of $M^2(\omega\eta_L)$ versus $M^2(\eta_H\eta_L)$ from the $\psi(3686)$ data.
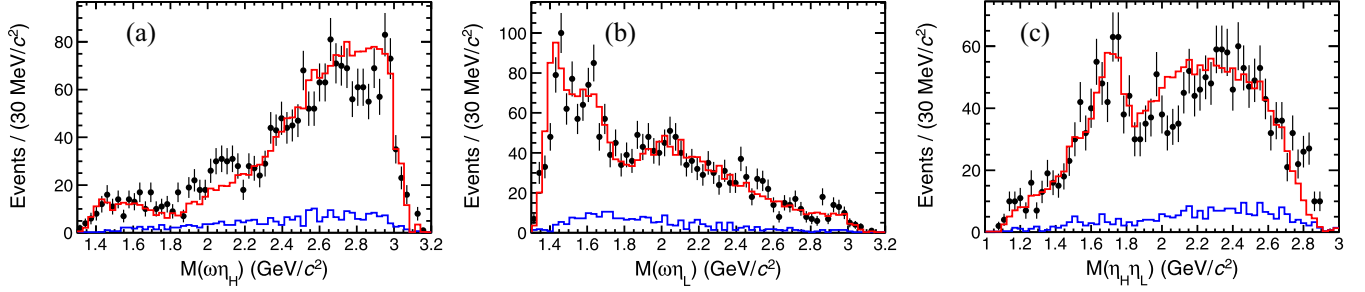
FIG. 4. The distributions of (a) $M(\omega\eta_H)$, (b) $M(\omega\eta_L)$, and (c) $M(\eta_H\eta_L)$, where the dots with error bars are the $\psi(3686)$ data, the red histogram shows the sum of the signal MC sample generated after the simplified partial wave analysis plus the ω sideband events in data, and the blue histogram shows the ω sideband events in data.

However, the measured significances and branching fractions for the intermediate states were found to vary substantially depending on the model components included. Due to this model dependence and the limited statistics, the PWA results are not reported. The amplitude model is used to extract the signal efficiency.

VI. SYSTEMATIC UNCERTAINTY

The sources of systematic uncertainty are the total $\psi(3686)$ event count, photon detection, pion tracking and PID, 4C kinematic fit, η mass window, MC model and statistics, photon miscombination, quoted branching fractions, $M(\pi^+\pi^-\pi^0)$ fit, and interference with continuum production. They are discussed below.

The uncertainty of the total number of $\psi(3686)$ events is estimated to be 0.5% [23]. The systematic uncertainty due to photon detection is estimated with the control sample of $J/\psi \to \rho\pi$ to be 1.0% for each photon [24]. The systematic uncertainty associated with the pion tracking is assigned as 1.0% for each π by using the control sample of $J/\psi \to \pi^+\pi^- p\bar{p}$ [24]. The systematic uncertainty due to the pion PID is assigned to be 1.0% for each pion by using the control sample of $J/\psi \to \pi^+\pi^-\pi^0$ [25]. The uncertainty related to the 4C kinematic fit is estimated by correcting the helix parameters of the simulated charged tracks to match data [23]. The difference between the signal efficiencies with and without correction is 0.03%, which is negligible.

The systematic uncertainties due to the difference in the mass resolutions and central value of mass between data and MC are estimated by fitting the mass spectrum with the MC shape convolved with a fixed-parameter Gaussian function, where the fixed parameters are extracted from a control sample of $\psi(3686) \to \omega\eta\eta'$. The change of the signal yield is taken as the systematic uncertainty. The uncertainties are obtained as 0.1% and 0.2%, respectively.

The uncertainty arising from the MC model is evaluated using an alternative amplitude model, while the quoted mass and width are smeared with their associated uncertainties. The relative difference in the detection efficiency, 2.9%, is taken as the uncertainty. The uncertainty due to

limited MC statistics is assigned to be 0.4% by $\frac{1}{\sqrt{N}}\sqrt{\frac{1-\varepsilon}{\varepsilon}}$, where ε is detection efficiency and N is total number of produced signal MC events.

For the uncertainty of photon miscombinations, we perform angle matching with truth information, considering a successful match within a range of five degrees. The calculated miscombination rate, 0.3%, is assigned as the systematic uncertainty. The systematic uncertainty related to the quoted branching fractions of $\omega \to \pi^+\pi^-\pi^0$, $\eta \to \gamma\gamma$, and $\pi^0 \to \gamma\gamma$ is assigned as 1.3% [4].

The systematic uncertainty introduced by the fit procedure includes the fit range of ω, the signal shape of the ω fit, and the background shape of the ω fit. To estimate the systematic uncertainty due to fit range, several alternative fits in different ranges ([0.64, 0.89] GeV/c^2, [0.66, 0.91] GeV/c^2, [0.64, 0.91] GeV/c^2, [0.66, 0.89] GeV/c^2) are performed. The largest resulting difference in the fit mass spectrum of ω is assigned as the systematic uncertainty, 2.1%. To estimate the uncertainty due to the signal shape, we replace the signal shape convolved with a free Gaussian function to a fixed Gaussian function; the difference between the fits before and after the change, 0.3%, is taken as the systematic uncertainty. For the systematic uncertainty due to the background shape, the difference of the fitted signal yields with and without the $\eta_H - \eta_L$ sideband shape, 4.3%, is taken as the systematic uncertainty. These three uncertainties are added in quadrature to obtain the systematic uncertainty due to the $M(\pi^+\pi^-\pi^0)$ fit. The systematic uncertainty of the interference with continuum production is investigated with the data sample taken at $\sqrt{s} = 3.773$ GeV based on the method described in Ref. [26]. The ratio of the impact from the interference term with respect to the resonance term is defined as:

$$r_R^f = \frac{2}{\hbar c} AB \sin\varphi, \text{ and } A = \sqrt{\frac{\sigma_c^f(s)}{\mathcal{B}_f}}, \text{ where } \hbar c \text{ is the con-}$$

version constant, $\sigma_c^f(s)$ is the cross section of the continuum production process, $\mathcal{B}_f$ is the branching fraction of $\psi(3686) \to \omega\eta\eta$ obtained in this analysis, and B is a constant depending on the resonance

TABLE I. Relative systematic uncertainties in the measurement of the branching fraction of $\psi(3686) \to \omega\eta\eta$.

Source	Uncertainty (%)
$N_{\psi(3686)}$	0.5
Photon detection	6.0
MDC tracking	2.0
PID	2.0
η mass window	0.2
MC model	2.9
MC statistics	0.4
Miscombination of photons	0.3
Quoted branching fractions	1.3
$M(\pi^+\pi^-\pi^0)$ fit	4.8
Interference with continuum production	9.2
Total	12.7

parameters quoted from Ref. [26]. $\sigma_c^f(s)$ is calculated by $\sigma_c^f(s) = \frac{N_{\text{con}}}{\mathcal{L}_{\psi(3770)}\epsilon\mathcal{B}} \times \frac{s_{3770}}{s_{3686}}$, where $N_{\text{con}} = 23.0 \pm 7.0$ represents the estimated yield of the continuum production, $\epsilon = 0.21$ is the detection efficiency for continuum production, $\mathcal{L}_{\psi(3770)} = 2.93 \text{ fb}^{-1}$ is the corresponding integrated luminosity, and s_{3770} and s_{3686} are the squares of the corresponding center-of-mass energies. $\mathcal{B}$ is the multiplicative result of branching fractions of $\omega \to \pi^+\pi^-\pi^0$, $\eta \to \gamma\gamma$, and $\pi^0 \to \gamma\gamma$ quoted from PDG [4]. We consider the $1/s$ dependency of the continuum contribution cross section and scale the cross section from $\sqrt{s} = 3.773$ GeV to $\sqrt{s} = 3.686$ GeV. For a conservative estimate, the difference in r_R^f between $\phi = 90°$ and $\phi = -90°$, 9.2%, is taken as the uncertainty. All of the above contributions are added in quadrature to obtain the total systematic uncertainty as shown in Table I.

VII. SUMMARY

Using $(2.712 \pm 0.014) \times 10^9$ $\psi(3686)$ events collected with the BESIII detector in 2009, 2012, and 2021, the decay $\psi(3686) \to \omega\eta\eta$ is observed for the first time. The branching fraction is measured to be $(1.65 \pm 0.02 \pm 0.21) \times 10^{-5}$, where the first uncertainty is statistical and the second systematic. However, due to limited statistics and significant interference effects, possible resonance such as excited h_1 or ω resonances cannot be identified. A future larger-statistics dataset, combined with theoretical input incorporating potential interference effects, could improve the understanding of the $\omega\eta$ and $\eta\eta$ systems.

DATA AVAILABILITY

The data that support the findings of this Letter are not publicly available. The data are available from the authors upon reasonable request.

[1] G. Toledo Sanchez and J. Piekarewicz, Phys. Rev. C **70**, 035206 (2004).

[2] R. A. Brambilla *et al.*, Chin. Phys. C **40**, 042001 (2016).

[3] N. Brambilla, S. Eidelman, B. K. Heltsley R. Vogt *et al.*, Eur. Phys. J. C **71**, 1534 (2011).

[4] S. Navas *et al.* (Particle Data Group), Phys. Rev. D **110**, 030001 (2024).

[5] M. Ablikim *et al.* (BESIII Collaboration), Phys. Rev. D **91**, 112008 (2015).

[6] M. Ablikim *et al.* (BESIII Collaboration), Chin. Phys. C **48**, 093001 (2024).

[7] M. Ablikim *et al.* (BESIII Collaboration), Nucl. Instrum. Methods Phys. Res., Sect. A **614**, 345 (2010).

[8] C. H. Yu *et al.*, *Proceedings of IPAC 2016* (JACoW, Busan, 2016).

[9] X. Li *et al.*, Radiat. Detect. Technol. Methods **1**, 13 (2017).

[10] Y. X. Guo *et al.*, Radiat. Detect. Technol. Methods **1**, 15 (2017).

[11] P. Cao *et al.*, Nucl. Instrum. Methods Phys. Res., Sect. A **953**, 163053 (2020).

[12] S. Agostinelli *et al.* (GEANT4 Collaboration), Nucl. Instrum. Methods Phys. Res., Sect. A **506**, 250 (2003).

[13] K. X. Huang *et al.*, Nucl. Sci. Tech. **33**, 142 (2022).

[14] S. Jadach, B. F. L. Ward, and Z. Was, Comput. Phys. Commun. **130**, 260 (2000).

[15] S. Jadach, B. F. L. Ward, and Z. Was, Phys. Rev. D **63**, 113009 (2001).

[16] R. G. Ping, Chin. Phys. C **32**, 599 (2008).

[17] D. J. Lange, Nucl. Instrum. Methods Phys. Res., Sect. A **462**, 152 (2001).

[18] J. C. Chen, G. S. Huang, X. R. Qi, D. H. Zhang, and Y. S. Zhu, Phys. Rev. D **62**, 034003 (2000).

[19] R. L. Yang, R. G. Ping, and H. Chen, Chin. Phys. Lett. **31**, 061301 (2014).

[20] E. Barberio, B. van Eijk, and Z. Was, Comput. Phys. Commun. **66**, 115 (1991).

[21] I. Antcheva *et al.*, Comput. Phys. Commun. **180**, 2499 (2009).

[22] B. S. Zou and D. V. Bugg, Eur. Phys. J. A **16**, 537 (2003).

[23] M. Ablikim *et al.* (BESIII Collaboration), Chin. Phys. C **42**, 023001 (2018).

[24] M. Ablikim *et al.* (BESIII Collaboration), Phys. Rev. D **83**, 112005 (2011).

[25] M. Ablikim *et al.* (BESIII Collaboration), Phys. Rev. D **85**, 092012 (2012).

[26] Y. P. Guo and C. Z. Yuan, Phys. Rev. D **105**, 114001 (2022).

[27] https://cstr.cn/31109.02.BEPC.

M. Ablikim,[1] M. N. Achasov,[4,c] P. Adlarson,[77] X. C. Ai,[82] R. Aliberti,[36] A. Amoroso,[76a,76c] Q. An,[73,59,a] Y. Bai,[58] O. Bakina,[37] Y. Ban,[47,h] H.-R. Bao,[65] V. Batozskaya,[1,45] K. Begzsuren,[33] N. Berger,[36] M. Berlowski,[45] M. Bertani,[29a] D. Bettoni,[30a] F. Bianchi,[76a,76c] E. Bianco,[76a,76c] A. Bortone,[76a,76c] I. Boyko,[37] R. A. Briere,[5] A. Brueggemann,[70] H. Cai,[78] M. H. Cai,[39,k,l] X. Cai,[1,59] A. Calcaterra,[29a] G. F. Cao,[1,65] N. Cao,[1,65] S. A. Cetin,[63a] X. Y. Chai,[47,h] J. F. Chang,[1,59] G. R. Che,[44] Y. Z. Che,[1,59,65] C. H. Chen,[9] Chao Chen,[56] G. Chen,[1] H. S. Chen,[1,65] H. Y. Chen,[21] M. L. Chen,[1,59,65] S. J. Chen,[43] S. L. Chen,[46] S. M. Chen,[62] T. Chen,[1,65] X. R. Chen,[32,65] X. T. Chen,[1,65] X. Y. Chen,[12,g] Y. B. Chen,[1,59] Y. Q. Chen,[35] Y. Q. Chen,[16] Z. Chen,[25] Z. J. Chen,[26,i] Z. K. Chen,[60] J. C. Cheng,[46] S. K. Choi,[10] X. Chu,[12,g] G. Cibinetto,[30a] F. Cossio,[76c] J. Cottee-Meldrum,[64] J. J. Cui,[51] H. L. Dai,[1,59] J. P. Dai,[80] A. Dbeyssi,[19] R. E. de Boer,[3] D. Dedovich,[37] C. Q. Deng,[74] Z. Y. Deng,[1] A. Denig,[36] I. Denysenko,[37] M. Destefanis,[76a,76c] F. De Mori,[76a,76c] B. Ding,[68,1] X. X. Ding,[47,h] Y. Ding,[35] Y. Ding,[41] Y. X. Ding,[31] J. Dong,[1,59] L. Y. Dong,[1,65] M. Y. Dong,[1,59,65] X. Dong,[78] M. C. Du,[1] S. X. Du,[12,g] S. X. Du,[82] Y. Y. Duan,[56] Z. H. Duan,[43] P. Egorov,[37,b] G. F. Fan,[43] J. J. Fan,[20] Y. H. Fan,[46] J. Fang,[1,59] J. Fang,[60] S. S. Fang,[1,65] W. X. Fang,[1] Y. Q. Fang,[1,59] L. Fava,[76b,76c] F. Feldbauer,[3] G. Felici,[29a] C. Q. Feng,[73,59] J. H. Feng,[16] L. Feng,[39,k,l] Q. X. Feng,[39,k,l] Y. T. Feng,[73,59] M. Fritsch,[3] C. D. Fu,[1] J. L. Fu,[65] Y. W. Fu,[1,65] H. Gao,[65] X. B. Gao,[42] Y. Gao,[73,59] Y. N. Gao,[47,h] Y. N. Gao,[20] Y. Y. Gao,[31] S. Garbolino,[76c] I. Garzia,[30a,30b] L. Ge,[58] P. T. Ge,[20] Z. W. Ge,[43] C. Geng,[60] E. M. Gersabeck,[69] A. Gilman,[71] K. Goetzen,[13] J. D. Gong,[35] L. Gong,[41] W. X. Gong,[1,59] W. Gradl,[36] S. Gramigna,[30a,30b] M. Greco,[76a,76c] M. H. Gu,[1,59] Y. T. Gu,[15] C. Y. Guan,[1,65] A. Q. Guo,[32] L. B. Guo,[42] M. J. Guo,[51] R. P. Guo,[50] Y. P. Guo,[12,g] A. Guskov,[37,b] J. Gutierrez,[28] K. L. Han,[65] T. T. Han,[1] F. Hanisch,[3] K. D. Hao,[73,59] X. Q. Hao,[20] F. A. Harris,[67] K. K. He,[56] K. L. He,[1,65] F. H. Heinsius,[3] C. H. Heinz,[36] Y. K. Heng,[1,59,65] C. Herold,[61] P. C. Hong,[35] G. Y. Hou,[1,65] X. T. Hou,[1,65] Y. R. Hou,[65] Z. L. Hou,[1] H. M. Hu,[1,65] J. F. Hu,[57,j] Q. P. Hu,[73,59] S. L. Hu,[12,g] T. Hu,[1,59,65] Y. Hu,[1] Z. M. Hu,[60] G. S. Huang,[73,59] K. X. Huang,[60] L. Q. Huang,[32,65] P. Huang,[43] X. T. Huang,[51] Y. P. Huang,[1] Y. S. Huang,[60] T. Hussain,[75] N. Hüsken,[36] N. in der Wiesche,[70] J. Jackson,[28] Q. Ji,[1] Q. P. Ji,[20] W. Ji,[1,65] X. B. Ji,[1,65] X. L. Ji,[1,59] Y. Y. Ji,[51] Z. K. Jia,[73,59] D. Jiang,[1,65] H. B. Jiang,[78] P. C. Jiang,[47,h] S. J. Jiang,[9] T. J. Jiang,[17] X. S. Jiang,[1,59,65] Y. Jiang,[65] J. B. Jiao,[51] J. K. Jiao,[35] Z. Jiao,[24] S. Jin,[43] Y. Jin,[68] M. Q. Jing,[1,65] X. M. Jing,[65] T. Johansson,[77] S. Kabana,[34] N. Kalantar-Nayestanaki,[66] X. L. Kang,[9] X. S. Kang,[41] M. Kavatsyuk,[66] B. C. Ke,[82] V. Khachatryan,[28] A. Khoukaz,[70] R. Kiuchi,[1] O. B. Kolcu,[63a] B. Kopf,[3] M. Kuessner,[3] X. Kui,[1,65] N. Kumar,[27] A. Kupsc,[45,77] W. Kühn,[38] Q. Lan,[74] W. N. Lan,[20] T. T. Lei,[73,59]

M. Lellmann,[36] T. Lenz,[36] C. Li,[44] C. Li,[48] C. H. Li,[40] C. K. Li,[21] D. M. Li,[82] F. Li,[1,59] G. Li,[1] H. B. Li,[1,65] H. J. Li,[20] H. N. Li,[57,j] Hui Li,[44] J. R. Li,[62] J. S. Li,[60] K. Li,[1] K. L. Li,[39,k,l] K. L. Li,[20] L. J. Li,[1,65] Lei Li,[49] M. H. Li,[44] M. R. Li,[1,65] P. L. Li,[65] P. R. Li,[39,k,l] Q. M. Li,[1,65] Q. X. Li,[51] R. Li,[18,32] S. X. Li,[12] T. Li,[51] T. Y. Li,[44] W. D. Li,[1,65] W. G. Li,[1,a] X. Li,[1,65] X. H. Li,[73,59] X. L. Li,[51] X. Y. Li,[1,8] X. Z. Li,[60] Y. Li,[20] Y. G. Li,[47,h] Y. P. Li,[35] Z. J. Li,[60] Z. Y. Li,[80] C. Liang,[43] H. Liang,[73,59] Y. F. Liang,[55] Y. T. Liang,[32,65] G. R. Liao,[14] L. B. Liao,[60] M. H. Liao,[60] Y. P. Liao,[1,65] J. Libby,[27] A. Limphirat,[61] C. C. Lin,[56] D. X. Lin,[32,65] L. Q. Lin,[40] T. Lin,[1] B. J. Liu,[1] B. X. Liu,[78] C. Liu,[35] C. X. Liu,[1] F. Liu,[1] F. H. Liu,[54] Feng Liu,[6] G. M. Liu,[57,j] H. Liu,[39,k,l] H. B. Liu,[15] H. H. Liu,[1] H. M. Liu,[1,65] Huihui Liu,[22] J. B. Liu,[73,59] J. J. Liu,[21] K. Liu,[39,k,l] K. Liu,[74] K. Y. Liu,[41] Ke Liu,[23] L. C. Liu,[44] Lu Liu,[44] M. H. Liu,[12,g] M. H. Liu,[35] P. L. Liu,[1] Q. Liu,[65] S. B. Liu,[73,59] T. Liu,[12,g] W. K. Liu,[44] W. M. Liu,[73,59] W. T. Liu,[40] X. Liu,[39,k,l] X. Liu,[40] X. K. Liu,[39,k,l] X. L. Liu,[12,g] X. Y. Liu,[78] Y. Liu,[82] Y. Liu,[82] Y. Liu,[39,k,l] Y. B. Liu,[44] Z. A. Liu,[1,59,65] Z. D. Liu,[9] Z. Q. Liu,[51] X. C. Lou,[1,59,65] F. X. Lu,[60] H. J. Lu,[24] J. G. Lu,[1,59] X. L. Lu,[16] Y. Lu,[7] Y. H. Lu,[1,65] Y. P. Lu,[1,59] Z. H. Lu,[1,65] C. L. Luo,[42] J. R. Luo,[60] J. S. Luo,[1,65] M. X. Luo,[81] T. Luo,[12,g] X. L. Luo,[1,59] Z. Y. Lv,[23] X. R. Lyu,[65,p] Y. F. Lyu,[44] Y. H. Lyu,[82] F. C. Ma,[41] H. L. Ma,[1] Heng Ma,[26,i] J. L. Ma,[1,65] L. L. Ma,[51] L. R. Ma,[68] Q. M. Ma,[1] R. Q. Ma,[1,65] R. Y. Ma,[20] T. Ma,[73,59] X. T. Ma,[1,65] X. Y. Ma,[1,59] Y. M. Ma,[32] F. E. Maas,[19] I. MacKay,[71] M. Maggiora,[76a,76c] S. Malde,[71] Q. A. Malik,[75] H. X. Mao,[39,k,l] Y. J. Mao,[47,h] Z. P. Mao,[1] S. Marcello,[76a,76c] A. Marshall,[64] F. M. Melendi,[30a,30b] Y. H. Meng,[65] Z. X. Meng,[68] G. Mezzadri,[30a] H. Miao,[1,65] T. J. Min,[43] R. E. Mitchell,[28] X. H. Mo,[1,59,65] B. Moses,[28] N. Yu. Muchnoi,[4,c] J. Muskalla,[36] Y. Nefedov,[37] F. Nerling,[19,e] L. S. Nie,[21] I. B. Nikolaev,[4,c] Z. Ning,[1,59] S. Nisar,[11,m] Q. L. Niu,[39,k,l] W. D. Niu,[12,g] C. Normand,[64] S. L. Olsen,[10,65] Q. Ouyang,[1,59,65] S. Pacetti,[29b,29c] X. Pan,[56] Y. Pan,[58] A. Pathak,[10] Y. P. Pei,[73,59] M. Pelizaeus,[3] H. P. Peng,[73,59] X. J. Peng,[39,k,l] Y. Y. Peng,[39,k,l] K. Peters,[13,e] K. Petridis,[64] J. L. Ping,[42] R. G. Ping,[1,65] S. Plura,[36] V. Prasad,[35] F. Z. Qi,[1] H. R. Qi,[62] M. Qi,[43] S. Qian,[1,59] W. B. Qian,[65] C. F. Qiao,[65] J. H. Qiao,[20] J. J. Qin,[74] J. L. Qin,[56] L. Q. Qin,[14] L. Y. Qin,[73,59] P. B. Qin,[74] X. P. Qin,[12,g] X. S. Qin,[51] Z. H. Qin,[1,59] J. F. Qiu,[1] Z. H. Qu,[74] J. Rademacker,[64] C. F. Redmer,[36] A. Rivetti,[76c] M. Rolo,[76c] G. Rong,[1,65] S. S. Rong,[1,65] F. Rosini,[29b,29c] Ch. Rosner,[19] M. Q. Ruan,[1,59] N. Salone,[45,q] A. Sarantsev,[37,d] Y. Schelhaas,[36] K. Schoenning,[77] M. Scodeggio,[30a] K. Y. Shan,[12,g] W. Shan,[25] X. Y. Shan,[73,59] Z. J. Shang,[39,k,l] J. F. Shangguan,[17] L. G. Shao,[1,65] M. Shao,[73,59] C. P. Shen,[12,g] H. F. Shen,[1,8] W. H. Shen,[65] X. Y. Shen,[1,65] B. A. Shi,[65] H. Shi,[73,59] J. L. Shi,[12,g] J. Y. Shi,[1] S. Y. Shi,[74] X. Shi,[1,59] H. L. Song,[73,59] J. J. Song,[20] T. Z. Song,[60] W. M. Song,[35] Y. J. Song,[12,g] Y. X. Song,[47,h,n] Zirong Song,[26,i] S. Sosio,[76a,76c] S. Spataro,[76a,76c] S. Stansilaus,[71] F. Stieler,[36] S. S. Su,[41] Y. J. Su,[65] G. B. Sun,[78] G. X. Sun,[1] H. Sun,[65] H. K. Sun,[1] J. F. Sun,[20] K. Sun,[62] L. Sun,[78] S. S. Sun,[1,65] T. Sun,[52,f] Y. C. Sun,[78] Y. H. Sun,[31] Y. J. Sun,[73,59] Y. Z. Sun,[1] Z. Q. Sun,[1,65] Z. T. Sun,[51] C. J. Tang,[55] G. Y. Tang,[1] J. Tang,[60] J. J. Tang,[73,59] L. F. Tang,[40] Y. A. Tang,[78] L. Y. Tao,[74] M. Tat,[71] J. X. Teng,[73,59] J. Y. Tian,[73,59] W. H. Tian,[60] Y. Tian,[32] Z. F. Tian,[78] I. Uman,[63b] B. Wang,[60] B. Wang,[1] Bo Wang,[73,59] C. Wang,[39,k,l] C. Wang,[20] Cong Wang,[23] D. Y. Wang,[47,h] H. J. Wang,[39,k,l] J. J. Wang,[78] K. Wang,[1,59] L. L. Wang,[1] L. W. Wang,[35] M. Wang,[51] M. Wang,[73,59] N. Y. Wang,[65] S. Wang,[12,g] T. Wang,[12,g] T. J. Wang,[44] W. Wang,[60] W. Wang,[74] W. P. Wang,[36] X. Wang,[47,h] X. F. Wang,[39,k,l] X. J. Wang,[40] X. L. Wang,[12,g] X. N. Wang,[1,65] Y. Wang,[62] Y. D. Wang,[46] Y. F. Wang,[1,8,65] Y. H. Wang,[39,k,l] Y. J. Wang,[73,59] Y. L. Wang,[20] Y. N. Wang,[78] Y. Q. Wang,[1] Yaqian Wang,[18] Yi Wang,[62] Yuan Wang,[18,32] Z. Wang,[1,59] Z. L. Wang,[2] Z. L. Wang,[74] Z. Q. Wang,[12,g] Z. Y. Wang,[1,65] D. H. Wei,[14] H. R. Wei,[44] F. Weidner,[70] S. P. Wen,[1] Y. R. Wen,[40] U. Wiedner,[3] G. Wilkinson,[71] M. Wolke,[77] C. Wu,[40] J. F. Wu,[1,8] L. H. Wu,[1] L. J. Wu,[1,65] L. J. Wu,[20] Lianjie Wu,[20] S. G. Wu,[1,65] S. M. Wu,[65] X. Wu,[12,g] X. H. Wu,[35] Y. J. Wu,[32] Z. Wu,[1,59] L. Xia,[73,59] X. M. Xian,[40] B. H. Xiang,[1,65] D. Xiao,[39,k,l] G. Y. Xiao,[43] H. Xiao,[74] Y. L. Xiao,[12,g] Z. J. Xiao,[42] C. Xie,[43] K. J. Xie,[1,65] X. H. Xie,[47,h] Y. Xie,[51] Y. G. Xie,[1,59] Y. H. Xie,[6] Z. P. Xie,[73,59] T. Y. Xing,[1,65] C. F. Xu,[1,65] C. J. Xu,[60] G. F. Xu,[1] H. Y. Xu,[2] H. Y. Xu,[68,2] M. Xu,[73,59] Q. J. Xu,[17] Q. N. Xu,[31] T. D. Xu,[74] W. Xu,[1] W. L. Xu,[68] X. P. Xu,[56] Y. Xu,[41] Y. Xu,[12,g] Y. C. Xu,[79] Z. S. Xu,[65] F. Yan,[12,g] H. Y. Yan,[40] L. Yan,[12,g] W. B. Yan,[73,59] W. C. Yan,[82] W. H. Yan,[6] W. P. Yan,[20] X. Q. Yan,[1,65] H. J. Yang,[52,f] H. L. Yang,[35] H. X. Yang,[1] J. H. Yang,[43] R. J. Yang,[20] T. Yang,[1] Y. Yang,[12,g] Y. F. Yang,[44] Y. H. Yang,[43] Y. Q. Yang,[9] Y. X. Yang,[1,65] Y. Z. Yang,[20] M. Ye,[1,59] M. H. Ye,[8,a] Z. J. Ye,[57,j] Junhao Yin,[44] Z. Y. You,[60] B. X. Yu,[1,59,65] C. X. Yu,[44] G. Yu,[13] J. S. Yu,[26,i] L. Q. Yu,[12,g] M. C. Yu,[41] T. Yu,[74] X. D. Yu,[47,h] Y. C. Yu,[82] C. Z. Yuan,[1,65] H. Yuan,[1,65] J. Yuan,[35] J. Yuan,[46] L. Yuan,[2] S. C. Yuan,[1,65] S. H. Yuan,[74] X. Q. Yuan,[1] Y. Yuan,[1,65] Z. Y. Yuan,[60] C. X. Yue,[40] Ying Yue,[20] A. A. Zafar,[75] S. H. Zeng,[64] X. Zeng,[12,g] Y. Zeng,[26,i] Y. J. Zeng,[1,65] Y. J. Zeng,[60] X. Y. Zhai,[35] Y. H. Zhan,[60] A. Q. Zhang,[1,65] B. L. Zhang,[1,65] B. X. Zhang,[1] D. H. Zhang,[44] G. Y. Zhang,[1,65] G. Y. Zhang,[20] H. Zhang,[82] H. Zhang,[73,59] H. C. Zhang,[1,59,65] H. H. Zhang,[60] H. Q. Zhang,[1,59,65] H. R. Zhang,[73,59] H. Y. Zhang,[1,59] J. Zhang,[60] J. Zhang,[82] J. J. Zhang,[53] J. L. Zhang,[21] J. Q. Zhang,[42] J. S. Zhang,[12,g] J. W. Zhang,[1,59,65] J. X. Zhang,[39,k,l] J. Y. Zhang,[1] J. Z. Zhang,[1,65] Jianyu Zhang,[65] L. M. Zhang,[62] Lei Zhang,[43] N. Zhang,[82] P. Zhang,[1,8] Q. Zhang,[20] Q. Y. Zhang,[35] R. Y. Zhang,[39,k,l] S. H. Zhang,[1,65]

Shulei Zhang,[26,i] X. M. Zhang,[1] X. Y. Zhang,[41] X. Y. Zhang,[51] Y. Zhang,[1] Y. Zhang,[74] Y. T. Zhang,[82] Y. H. Zhang,[1,59] Y. M. Zhang,[40] Y. P. Zhang,[73,59] Z. D. Zhang,[1] Z. H. Zhang,[1] Z. L. Zhang,[35] Z. L. Zhang,[56] Z. X. Zhang,[20] Z. Y. Zhang,[78] Z. Y. Zhang,[44] Z. Z. Zhang,[46] Zh. Zh. Zhang,[20] G. Zhao,[1] J. Y. Zhao,[1,65] J. Z. Zhao,[1,59] L. Zhao,[1] L. Zhao,[73,59] M. G. Zhao,[44] N. Zhao,[80] R. P. Zhao,[65] S. J. Zhao,[82] Y. B. Zhao,[1,59] Y. L. Zhao,[56] Y. X. Zhao,[32,65] Z. G. Zhao,[73,59] A. Zhemchugov,[37,b] B. Zheng,[74] B. M. Zheng,[35] J. P. Zheng,[1,59] W. J. Zheng,[1,65] X. R. Zheng,[20] Y. H. Zheng,[65,p] B. Zhong,[42] C. Zhong,[20] H. Zhou,[36,51,o] J. Q. Zhou,[35] J. Y. Zhou,[35] S. Zhou,[6] X. Zhou,[78] X. K. Zhou,[6] X. R. Zhou,[73,59] X. Y. Zhou,[40] Y. X. Zhou,[79] Y. Z. Zhou,[12,g] A. N. Zhu,[65] J. Zhu,[44] K. Zhu,[1] K. J. Zhu,[1,59,65] K. S. Zhu,[12,g] L. Zhu,[35] L. X. Zhu,[65] S. H. Zhu,[72] T. J. Zhu,[12,g] W. D. Zhu,[12,g] W. D. Zhu,[42] W. J. Zhu,[1] W. Z. Zhu,[20] Y. C. Zhu,[73,59] Z. A. Zhu,[1,65] X. Y. Zhuang,[44] J. H. Zou,[1] and J. Zu[73,59]

(BESIII Collaboration)

[1]*Institute of High Energy Physics, Beijing 100049, People's Republic of China*
[2]*Beihang University, Beijing 100191, People's Republic of China*
[3]*Bochum Ruhr-University, D-44780 Bochum, Germany*
[4]*Budker Institute of Nuclear Physics SB RAS (BINP), Novosibirsk 630090, Russia*
[5]*Carnegie Mellon University, Pittsburgh, Pennsylvania 15213, USA*
[6]*Central China Normal University, Wuhan 430079, People's Republic of China*
[7]*Central South University, Changsha 410083, People's Republic of China*
[8]*China Center of Advanced Science and Technology, Beijing 100190, People's Republic of China*
[9]*China University of Geosciences, Wuhan 430074, People's Republic of China*
[10]*Chung-Ang University, Seoul, 06974, Republic of Korea*
[11]*COMSATS University Islamabad,*
Lahore Campus, Defence Road, Off Raiwind Road, 54000 Lahore, Pakistan
[12]*Fudan University, Shanghai 200433, People's Republic of China*
[13]*GSI Helmholtzcentre for Heavy Ion Research GmbH, D-64291 Darmstadt, Germany*
[14]*Guangxi Normal University, Guilin 541004, People's Republic of China*
[15]*Guangxi University, Nanning 530004, People's Republic of China*
[16]*Guangxi University of Science and Technology, Liuzhou 545006, People's Republic of China*
[17]*Hangzhou Normal University, Hangzhou 310036, People's Republic of China*
[18]*Hebei University, Baoding 071002, People's Republic of China*
[19]*Helmholtz Institute Mainz, Staudinger Weg 18, D-55099 Mainz, Germany*
[20]*Henan Normal University, Xinxiang 453007, People's Republic of China*
[21]*Henan University, Kaifeng 475004, People's Republic of China*
[22]*Henan University of Science and Technology, Luoyang 471003, People's Republic of China*
[23]*Henan University of Technology, Zhengzhou 450001, People's Republic of China*
[24]*Huangshan College, Huangshan 245000, People's Republic of China*
[25]*Hunan Normal University, Changsha 410081, People's Republic of China*
[26]*Hunan University, Changsha 410082, People's Republic of China*
[27]*Indian Institute of Technology Madras, Chennai 600036, India*
[28]*Indiana University, Bloomington, Indiana 47405, USA*
[29a]*INFN Laboratori Nazionali di Frascati, I-00044, Frascati, Italy*
[29b]*INFN Sezione di Perugia, I-06100, Perugia, Italy*
[29c]*University of Perugia, I-06100, Perugia, Italy*
[30a]*INFN Sezione di Ferrara, I-44122, Ferrara, Italy*
[30b]*University of Ferrara, I-44122, Ferrara, Italy*
[31]*Inner Mongolia University, Hohhot 010021, People's Republic of China*
[32]*Institute of Modern Physics, Lanzhou 730000, People's Republic of China*
[33]*Institute of Physics and Technology, Mongolian Academy of Sciences,*
Peace Avenue 54B, Ulaanbaatar 13330, Mongolia
[34]*Instituto de Alta Investigación, Universidad de Tarapacá, Casilla 7D, Arica 1000000, Chile*
[35]*Jilin University, Changchun 130012, People's Republic of China*
[36]*Johannes Gutenberg University of Mainz, Johann-Joachim-Becher-Weg 45, D-55099 Mainz, Germany*
[37]*Joint Institute for Nuclear Research, 141980 Dubna, Moscow region, Russia*
[38]*Justus-Liebig-Universitaet Giessen, II. Physikalisches Institut,*
Heinrich-Buff-Ring 16, D-35392 Giessen, Germany
[39]*Lanzhou University, Lanzhou 730000, People's Republic of China*
[40]*Liaoning Normal University, Dalian 116029, People's Republic of China*

[41]Liaoning University, Shenyang 110036, People's Republic of China

[42]Nanjing Normal University, Nanjing 210023, People's Republic of China

[43]Nanjing University, Nanjing 210093, People's Republic of China

[44]Nankai University, Tianjin 300071, People's Republic of China

[45]National Centre for Nuclear Research, Warsaw 02-093, Poland

[46]North China Electric Power University, Beijing 102206, People's Republic of China

[47]Peking University, Beijing 100871, People's Republic of China

[48]Qufu Normal University, Qufu 273165, People's Republic of China

[49]Renmin University of China, Beijing 100872, People's Republic of China

[50]Shandong Normal University, Jinan 250014, People's Republic of China

[51]Shandong University, Jinan 250100, People's Republic of China

[52]Shanghai Jiao Tong University, Shanghai 200240, People's Republic of China

[53]Shanxi Normal University, Linfen 041004, People's Republic of China

[54]Shanxi University, Taiyuan 030006, People's Republic of China

[55]Sichuan University, Chengdu 610064, People's Republic of China

[56]Soochow University, Suzhou 215006, People's Republic of China

[57]South China Normal University, Guangzhou 510006, People's Republic of China

[58]Southeast University, Nanjing 211100, People's Republic of China

[59]State Key Laboratory of Particle Detection and Electronics,
Beijing 100049, Hefei 230026, People's Republic of China

[60]Sun Yat-Sen University, Guangzhou 510275, People's Republic of China

[61]Suranaree University of Technology, University Avenue 111, Nakhon Ratchasima 30000, Thailand

[62]Tsinghua University, Beijing 100084, People's Republic of China

[63a]Turkish Accelerator Center Particle Factory Group, Istinye University, 34010, Istanbul, Turkey

[63b]Near East University, Nicosia, North Cyprus, 99138, Mersin 10, Turkey

[64]University of Bristol, H H Wills Physics Laboratory, Tyndall Avenue, Bristol, BS8 1TL, United Kingdom

[65]University of Chinese Academy of Sciences, Beijing 100049, People's Republic of China

[66]University of Groningen, NL-9747 AA Groningen, The Netherlands

[67]University of Hawaii, Honolulu, Hawaii 96822, USA

[68]University of Jinan, Jinan 250022, People's Republic of China

[69]University of Manchester, Oxford Road, Manchester, M13 9PL, United Kingdom

[70]University of Muenster, Wilhelm-Klemm-Strasse 9, 48149 Muenster, Germany

[71]University of Oxford, Keble Road, Oxford OX13RH, United Kingdom

[72]University of Science and Technology Liaoning, Anshan 114051, People's Republic of China

[73]University of Science and Technology of China, Hefei 230026, People's Republic of China

[74]University of South China, Hengyang 421001, People's Republic of China

[75]University of the Punjab, Lahore-54590, Pakistan

[76a]University of Turin and INFN, University of Turin, I-10125, Turin, Italy

[76b]University of Eastern Piedmont, I-15121, Alessandria, Italy

[76c]INFN, I-10125, Turin, Italy

[77]Uppsala University, Box 516, SE-75120 Uppsala, Sweden

[78]Wuhan University, Wuhan 430072, People's Republic of China

[79]Yantai University, Yantai 264005, People's Republic of China

[80]Yunnan University, Kunming 650500, People's Republic of China

[81]Zhejiang University, Hangzhou 310027, People's Republic of China

[82]Zhengzhou University, Zhengzhou 450001, People's Republic of China

[a]Deceased.

[b]Also at the Moscow Institute of Physics and Technology, Moscow 141700, Russia.

[c]Also at the Novosibirsk State University, Novosibirsk, 630090, Russia.

[d]Also at the NRC "Kurchatov Institute," PNPI, 188300, Gatchina, Russia.

[e]Also at Goethe University Frankfurt, 60323 Frankfurt am Main, Germany.

[f]Also at Key Laboratory for Particle Physics, Astrophysics and Cosmology, Ministry of Education; Shanghai Key Laboratory for Particle Physics and Cosmology; Institute of Nuclear and Particle Physics, Shanghai 200240, People's Republic of China.

[g]Also at Key Laboratory of Nuclear Physics and Ion-beam Application (MOE) and Institute of Modern Physics, Fudan University, Shanghai 200443, People's Republic of China.

[h]Also at State Key Laboratory of Nuclear Physics and Technology, Peking University, Beijing 100871, People's Republic of China.

[i]Also at School of Physics and Electronics, Hunan University, Changsha 410082, China.

[j]Also at Guangdong Provincial Key Laboratory of Nuclear Science, Institute of Quantum Matter, South China Normal University, Guangzhou 510006, China.

[k]Also at MOE Frontiers Science Center for Rare Isotopes, Lanzhou University, Lanzhou 730000, People's Republic of China.
[l]Also at Lanzhou Center for Theoretical Physics, Lanzhou University, Lanzhou 730000, People's Republic of China.
[m]Also at the Department of Mathematical Sciences, IBA, Karachi 75270, Pakistan.
[n]Also at Ecole Polytechnique Federale de Lausanne (EPFL), CH-1015 Lausanne, Switzerland.
[o]Also at Helmholtz Institute Mainz, Staudinger Weg 18, D-55099 Mainz, Germany.
[p]Also at Hangzhou Institute for Advanced Study, University of Chinese Academy of Sciences, Hangzhou 310024, China.
[q]Present address: Silesian University in Katowice, Chorzow, 41-500, Poland.